




Test-retest repeatability of organ uptake on PSMA-targeted 18F-DCFPyL PET/CT in patients with prostate cancer

Rudolf A. Werner, Susanne Lütje, Bilêl Habacha, Lena Bundschuh, Takahiro Higuchi, Andreas K. Buck, Aleksander Kosmala, Constantin Lapa, Markus Essler, Martin A. Lodge, Kenneth J. Pienta, Mario A. Eisenberger, Mark C. Markowski, Michael A. Gorin, Martin G. Pomper, Steven P. Rowe, Ralph Alexander Bundschuh

Angaben zur Veröffentlichung / Publication details:

Werner, Rudolf A., Susanne Lütje, Bilêl Habacha, Lena Bundschuh, Takahiro Higuchi, Andreas K. Buck, Aleksander Kosmala, et al. 2023. "Test-retest repeatability of organ uptake on PSMA-targeted 18F-DCFPyL PET/CT in patients with prostate cancer." *The Prostate* 83 (12): 1186–92.
<https://doi.org/10.1002/pros.24577>.

Test-retest repeatability of organ uptake on PSMA-targeted ^{18}F -DCFPyL PET/CT in patients with prostate cancer

Rudolf A. Werner MD^{1,2}  | Susanne Lütje MD³ | Bilél Habacha⁴ |
 Lena Bundschuh MSc⁵ | Takahiro Higuchi MD, PhD^{1,6} | Andreas K. Buck MD¹ |
 Aleksander Kosmala MD¹ | Constantin Lapa MD⁵ | Markus Essler MD⁴ |
 Martin A. Lodge PhD² | Kenneth J. Pienta MD⁷ | Mario A. Eisenberger MD⁸ |
 Mark C. Markowski MD⁸  | Michael A. Gorin⁹ | Martin G. Pomper MD² |
 Steven P. Rowe MD, PhD²  | Ralph A. Bundschuh MD, PhD⁵

¹Department of Nuclear Medicine, University Hospital Würzburg, Würzburg, Germany

²The Russell H. Morgan Department of Radiology and Radiological Science, Johns Hopkins University School of Medicine, Baltimore, Maryland, USA

³Department of Nuclear Medicine, University Hospital Aachen, Aachen, Germany

⁴Department of Nuclear Medicine, University Hospital Bonn, Bonn, Germany

⁵Nuclear Medicine, Faculty of Medicine, University of Augsburg, Augsburg, Germany

⁶Faculty of Medicine, Dentistry and Pharmaceutical Sciences, Okayama University, Okayama, Japan

⁷The James Buchanan Brady Urological Institute and Department of Urology, Johns Hopkins University School of Medicine, Baltimore, Maryland, USA

⁸Sidney Kimmel Comprehensive Cancer Center, Johns Hopkins University School of Medicine, Baltimore, Maryland, USA

⁹Milton and Carroll Petrie Department of Urology, Icahn School of Medicine at Mount Sinai, New York, New York, USA

Correspondence

Ralph A. Bundschuh, MD, PhD, Department of Nuclear Medicine, University Hospital Augsburg, Stenglinstr. 2, Augsburg 86156, Germany.
 Email: ralph.bundschuh@uni-a.de

Abstract

Objectives: We evaluated ^{18}F -DCFPyL test-retest repeatability of uptake in normal organs.

Methods: Twenty-two prostate cancer (PC) patients underwent two ^{18}F -DCFPyL PET scans within 7 days within a prospective clinical trial (NCT03793543). In both PET scans, uptake in normal organs (kidneys, spleen, liver, and salivary and lacrimal glands) was quantified. Repeatability was determined by using within-subject coefficient of variation (wCOV), with lower values indicating improved repeatability.

Results: For SUV_{mean} , repeatability was high for kidneys, spleen, liver, and parotid glands (wCOV, range: 9.0%–14.3%) and lower for lacrimal (23.9%) and submandibular glands (12.4%). For SUV_{max} , however, the lacrimal (14.4%) and submandibular glands (6.9%) achieved higher repeatability, while for large organs (kidneys, liver, spleen, and parotid glands), repeatability was low (range: 14.1%–45.2%).

Conclusion: We found acceptable repeatability of uptake on ^{18}F -DCFPyL PET for normal organs, in particular for SUV_{mean} in the liver or parotid glands. This may have implications for both PSMA-targeted imaging and treatment, as patient selection for radioligand therapy and standardized frameworks for scan interpretation (PROMISE, E-PSMA) rely on uptake in those reference organs.

KEYWORDS

^{18}F -DCFPyL, E-PSMA, organ uptake, PROMISE, prostate cancer, PSMA-PET/CT, radioligand therapy, theranostics

Steven P. Rowe and Ralph A. Bundschuh contributed equally to this study.

This is an open access article under the terms of the Creative Commons Attribution-NonCommercial-NoDerivs License, which permits use and distribution in any medium, provided the original work is properly cited, the use is non-commercial and no modifications or adaptations are made.

© 2023 The Authors. *The Prostate* published by Wiley Periodicals LLC.

1 | INTRODUCTION

Prostate-specific membrane antigen (PSMA)-directed ligands are frequently utilized in patients with prostate carcinoma (PC),¹ in particular, after recent approval for imaging by the US Food and Drug Administration (FDA).² Given the increasing number of scans in clinical routine, standardized reporting frameworks including PSMA reporting and data system (RADS),³ E-PSMA,⁴ and PROMISE⁵ may be used for scan interpretation. Those scoring systems achieve high interobserver agreement rates, even for inexperienced readers.⁶

For PROMISE, molecular imaging expression scores (miPSMA) are defined in relation to uptake derived from reference organs, for example, in the liver, parotid gland, or spleen. E-PSMA also relies on radiotracer accumulation in normal organs using the visual PSMA expression score, a 4-point scale including uptake relative to the liver and salivary glands.⁴ Recently, the PSMA PET tumor-to-Salivary Glands ratio (PSG score) was introduced. This metric, based on normal organ uptake in the parotid glands, may also be helpful to identify high-risk individuals scheduled for PSMA-targeted radioligand therapy (RLT).⁷

Despite its use to assign lesions attributable to PC and for patient selection before RLT, data on repeatability of normal organs is rather limited in the context of PSMA PET. For instance, Pollard and colleagues included 18 men imaged with ⁶⁸Ga-PSMA-11 and determined repeatability of tumor and normal tissue in a retrospective setting.⁸ In this study, within-subject coefficient of variation (wCOV) values for salivary glands and spleen were found to be 8.9% and 10.7%, respectively,⁸ thereby indicating high repeatability on ⁶⁸Ga-labeled PSMA PET. For ¹⁸F-labeled PSMA radiotracers, in particular for the FDA approved agent ¹⁸F-DCFPyL, quantitative test-retest data are still lacking, as recent studies only focused on tumor repeatability.^{9,10} Therefore, we examined the repeatability of radiotracer accumulation in normal organs on ¹⁸F-DCFPyL PET in a prospective test-retest setting, including liver, spleen, kidneys, and salivary and lacrimal glands.

2 | MATERIALS AND METHODS

2.1 | Patients and study design

Twenty-two patients (mean age 65.4 ± 9.4 years) with known PC were enrolled in this prospective trial which was registered at [ClinicalTrials.gov](https://clinicaltrials.gov) (identifier NCT03793543) and carried out under the auspices of a US FDA Investigational New Drug application (IND121064)¹¹ before FDA approval. The trial was approved by the institutional review board at the Johns Hopkins Hospital (IRB00174393). Twenty-one patients of this cohort were previously evaluated in Werner et al.¹⁰ to determine test-retest repeatability in sites of disease, but without assessing uptake in normal organs. The 22nd patient could not be included in the previous analysis as no PSMA-positive lesions had been found, but could be included for the present examination focusing on normal organ uptake.

Among all patients, original Gleason score ranged between 7 and 10 with a mean of 8. Serum PSA ranged between 0.4 and 138.4 ng/mL with a mean of 21.0 ng/mL. Consecutively, two ¹⁸F-DCFPyL PET/CT scans were performed within 7 days (mean 3.7 days, range 1–7 days). Between the two scans, no tumor-specific treatment was applied to any of the patients. For further details on inclusion or exclusion criteria and patient characteristics, please refer to Werner et al.¹⁰

2.2 | Imaging procedure

PET/CT was performed on a Siemens Biograph 128-slice mCT (Siemens Healthineers). Approximately 60 min (range 57–63 min) after the intravenous injection of mean 322.4 MBq for the first scan and 323.6 MBq for the second scan, PET data were acquired over 6–8 bed positions from the mid-thighs to the skull vertex (3 min per bed position) as well as a low-dose CT for attenuation correction. ¹⁸F-DCFPyL was produced as described in Szabo et al.¹² PET data were reconstructed using the standard clinical ordered subset expectation maximization algorithm implemented by the manufacturer including scatter and attenuation corrections based on the acquired low-dose CT. Details on imaging procedures can also be found in Werner et al.¹⁰

2.3 | Organ delineation

In both studies, the kidneys, the liver, the spleen as well as the lacrimal glands, the parotid glands, and the submandibular glands were delineated. For liver, spleen, and kidneys, CT data of the low-dose CT was used for organ segmentation after co-registration between PET and CT had been double-checked. Therefore, a semi-automatic model-based segmentation algorithm was used. After automatic pre-segmentation, a manual adaption was performed if necessary, especially in context with PET data. The segmentation of the salivary and lacrimal glands was based on the PET images by using a semi-automatic region-grow algorithm. After segmentation, maximum and mean standardized uptake values (SUV_{max/mean}) within the segmented volumes (VOIs) were derived. Procedures were carried out by two board-certified nuclear medicine physicians with long-standing experience in PET/CT imaging (Ralph A. Bundschuh and Susanne Lütje) using the Imanytics software (Version 3.2 rev. 6515, Philipps Research). We also assessed the repeatability of tumor-to-organ ratios by using the qPSG_{mean}, as provided in Hotta et al.⁷ by using a target lesion (TL). Moreover, the qPSG_{max}, defined as SUV_{max} of TL/SUV_{max} of parotid glands was also derived.

2.4 | Statistical analysis

Organ uptake was compared between the two scans. Scatter diagrams were plotted and linear regression analysis was performed for all organs. For paired organs, averaged values were calculated. Bland-Altman plots were created for the absolute and relative differences (expressed as %),

including upper and lower level of agreement. In addition, Kendall's tau (τ , ≥ 0.40 indicating good correlation) and within-patient coefficient of variation (wCOV, with lower values indicating improved repeatability) were also calculated. Statistical analysis was performed using the MedCalc software package (Version 19.6, MedCalc software Ltd.) as well as Microsoft Excel 2016 (Microsoft Cooperation). For further details, refer to Werner et al.¹⁰

3 | RESULTS

Organs of 22 patients were segmented on both scans (with the exception of lacrimal glands in one case which were not visible on the PET). A respective case displaying segmented normal organs is shown

in Figure 1, demonstrating virtually no uptake differences in unaffected organs on visual inspection in a test-retest setting. A target tumor lesion was segmented in 21 patients as one patient did not show any pathological finding.

SUV_{mean} achieved best repeatability for large organs, including kidneys, liver, spleen, and parotid glands. On the test scan, SUV_{mean} in normal organs was lowest for the spleen (5.0 ± 2.0), followed by the liver (5.5 ± 1.2), lacrimal glands (6.3 ± 2.2), parotid glands (9.6 ± 2.9), submandibular glands (10.2 ± 3.9) and kidneys (27.0 ± 10.4), with comparable results for all organs on retest PETs (Table 1).

Among all applied statistical tests, SUV_{mean} demonstrated best repeatability in larger organs (kidneys, liver, spleen). First, r values were high for large organs when SUV_{mean} was investigated (Figure 2, first columns), with 0.95 for kidneys and spleen, respectively, and

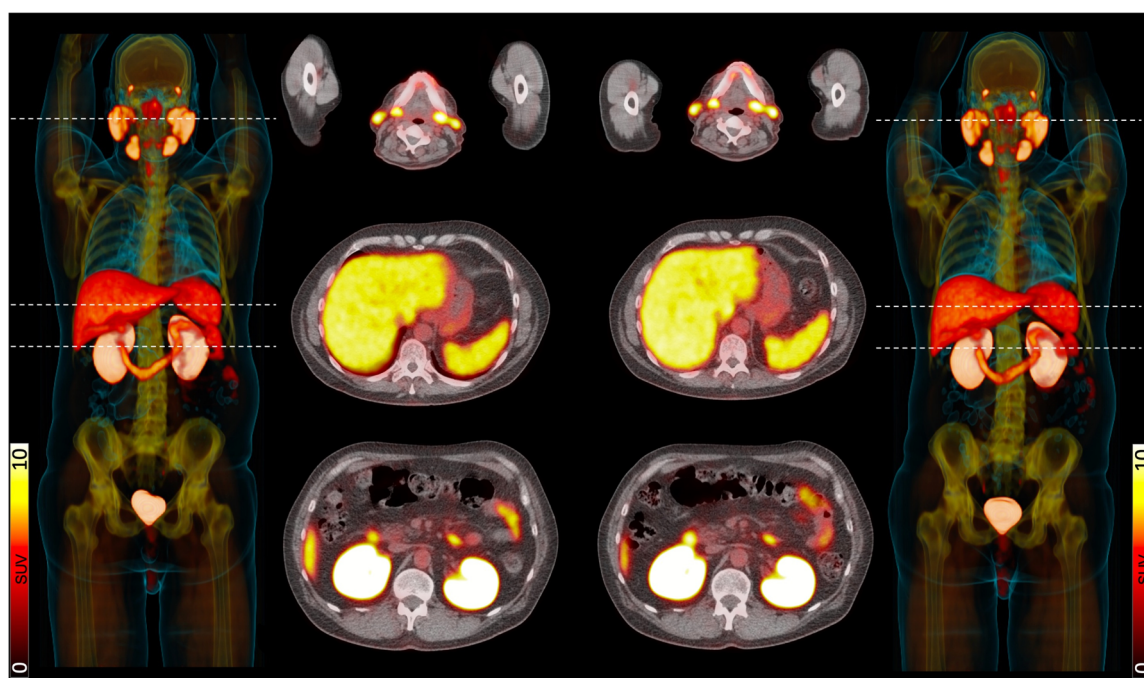


FIGURE 1 Patient affected with prostate cancer and imaged with ^{18}F -DCFPyL. Maximum intensity projection and transaxial PET/CTs provide an overview of all normal organs (liver, kidneys, spleen, lacrimal, and salivary glands) exhibiting physiological uptake on a test (left) and retest scan (right). Transaxial PET/CT shows intense radiotracer accumulation in the parotid glands (top), in the liver and spleen (middle), and in the kidneys (bottom). Visual assessment revealed virtually no uptake differences in any of the investigated organs.

TABLE 1 Mean standardized uptake values (SUV_{mean} , given as mean \pm standard deviation) derived from the test and retest scans, correlation coefficients, within-subject coefficient of variation (wCOV, given in %) and Kendall's τ for all normal organs of interest.

Organ	SUV_{mean} test	SUV_{mean} retest	r	wCOV	τ
Kidneys ($n = 44$)	27.0 ± 10.4	28.2 ± 11.1	0.95	9.1	0.81
Liver ($n = 22$)	5.5 ± 1.2	5.1 ± 1.9	0.87	9.0	0.74
Spleen ($n = 22$)	5.0 ± 2.0	5.4 ± 1.3	0.95	10.6	0.67
Gll. parotidae ($n = 44$)	9.6 ± 2.9	9.3 ± 2.6	0.77	14.3	0.58
Gll. lacrimalis ($n = 42$)*	6.3 ± 2.2	6.2 ± 1.5	0.36	23.9	0.44
Gll. submandibulares ($n = 44$)	10.2 ± 3.9	10.9 ± 4.1	0.91	12.4	0.73

Note: * indicates not assessable in one subject.

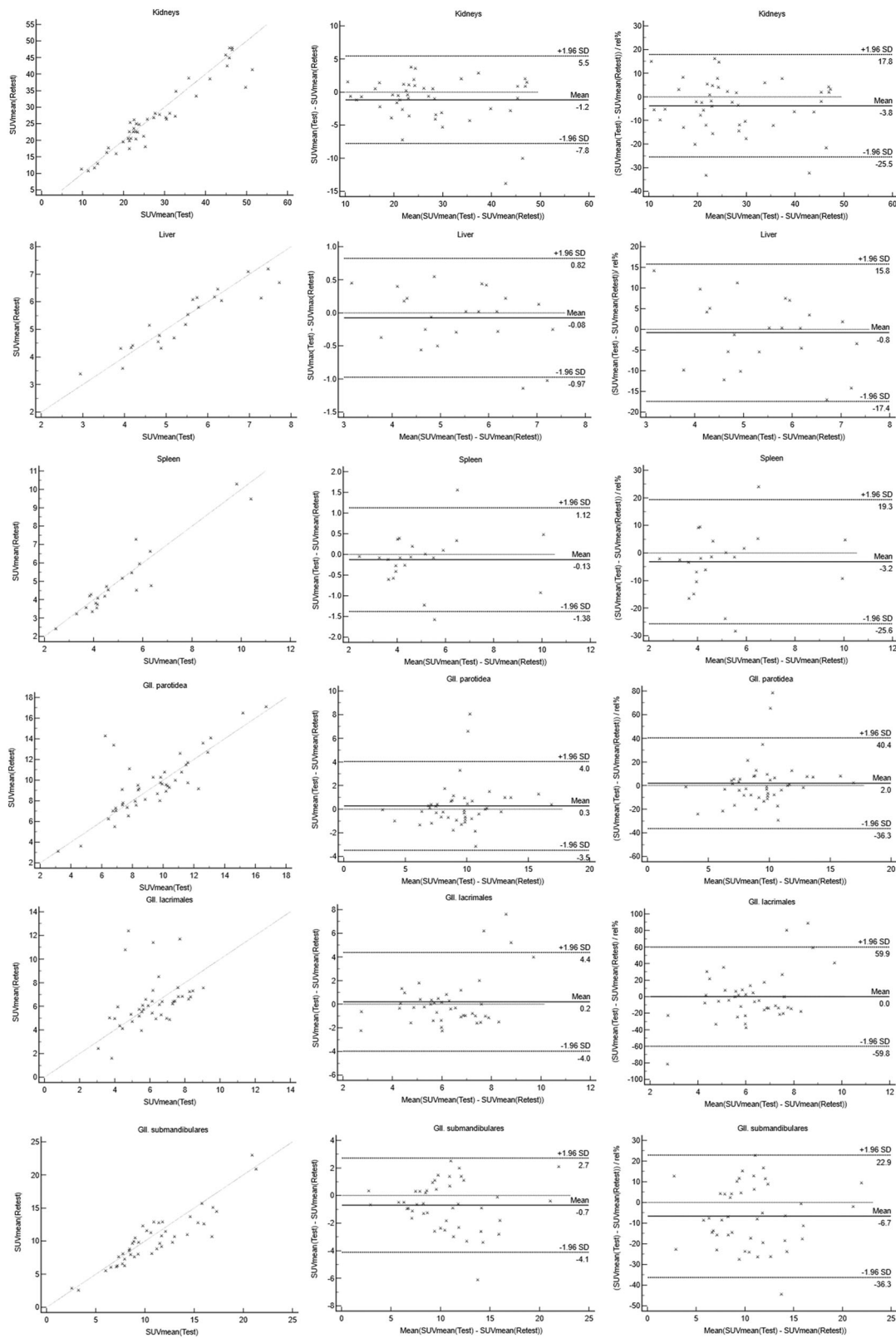


FIGURE 2 Correlations (first column), Bland-Altman plots for absolute (second column) and relative values (third column) of uptake in normal organs for mean standardized uptake values (SUV_{mean}). First row displays the kidneys, second row the liver, third row the spleen, fourth row the lacrimal, fifth row the parotid, and last row the submandibular glands. Correlations were excellent for all organs. For the liver and spleen, absolute and relative values demonstrated smaller magnitude of limits, when compared to the lacrimal, parotid, or submandibular glands.

0.87 for the spleen. For gland assessment, however, a broad range of r values were noted, ranging from 0.36 for lacrimal to 0.91 for submandibular glands. Second, wCOVs were 9.0% for the liver, 9.1% for the kidneys, and 10.6% for the spleen, followed by parotid glands (14.3%). Repeatability, however, was substantially lower for submandibular (12.4%), and lacrimal glands (23.9%). Last, similar results were recorded for τ , ranging from 0.44 for the latter organs to 0.81 for the kidneys. On Bland Altman plots for SUV_{mean} (Figure 2), there was no systematic increase or decrease for any of the investigated organs, with lowest ± 1.96 SD achieved for the liver (0.82%/–0.97%). For relative differences, SUV_{mean} showed larger magnitude of limits in all glands, with the largest interval in lacrimal glands (± 1.96 SD: 59.9%/–59.8%).

SUV_{max} achieved best repeatability for salivary and lacrimal glands. For SUV_{max} test scans achieved lowest uptake in lacrimal glands (12.6 ± 5.1), followed by spleen (15.9 ± 14.3) and the parotid (18.1 ± 8.3) and submandibular glands (19.3 ± 8.0). Highest SUV_{max} was recorded in the liver (20.4 ± 16.4), and kidneys (55.4 ± 18.8). Derived values on retest scans were almost identical (Table 2). Relative to SUV_{mean} , opposite findings for SUV_{max} were noted, with best repeatability recorded for smaller gland assessment. Higher r values were observed for investigated uptake in lacrimal ($r = 0.87$) and submandibular glands ($r = 0.98$), while larger organs exhibited lower r (≥ 0.66). Similar findings were recorded for wCOV (submandibular glands, 6.9%, indicating good repeatability vs. liver, 47%) and for τ , ranging from 0.55 for the liver to 0.83 for the submandibular glands. On Bland Altman plots for SUV_{max} (Figure 3), there was again no systematic increase or decrease, with lowest ± 1.96 SD achieved for the submandibular glands (4.2%/–3.2%). For relative differences, the largest magnitude of limits was recorded in the liver with a ± 1.96 SD of 112.4%/–92.6%.

$qPSG_{max}$ and $qPSG_{mean}$ achieved good repeatability as well. For $qPSG_{max}$, r was 0.97; wCOV, 12.3, and τ was 0.82, respectively. For $qPSG_{mean}$, comparable results were achieved, with r is 0.98; wCOV, 14.4, and τ , 0.79.

4 | DISCUSSION

Assessing the uptake in normal organs on the now-FDA-approved PET agent ^{18}F -DCFPyL, we observed high repeatability of radiotracer accumulation. For SUV_{mean} , we observed acceptable

repeatability for larger organs, including the spleen, liver, and kidneys (wCOV, 9%–10.6%), while smaller glands (lacrimal and submandibular glands) showed higher wCOV, indicating worse repeatability. For SUV_{max} , however, opposite findings were recorded, with best repeatability for submandibular glands (wCOV, 6.9%). As such, SUV_{mean} may be the preferred metric for larger organs, such as the liver, while for lacrimal and submandibular glands, SUV_{max} should be determined. For parotid glands, however, repeatability was comparable, but slightly improved for SUV_{mean} (14.3% vs. SUV_{max} , 18.5%). This may be of importance for standardized reporting, where those organs are routinely assessed to determine the likelihood of tumor lesions being attributable to PC, for example, the PROMISE-based miPSMA score with the liver serving as reference organ.⁵ In this regard, both academic and nonacademic users of such systems can then have certainty that scores based on normal organs would be repeatable.

Beyond its use for standardized reporting frameworks,^{4,5} quantification of normal organ uptake on baseline PSMA PET has also been recently suggested in the context of patient selection for RLT using ^{177}Lu -labeled PSMA agents. Hotta and coworkers introduced the PSG score, which uses the parotid glands as reference instead of the liver. In this regard, a visual assessment (vPSG) and a quantitative scoring (qPSG) can be applied, which is a ratio of the SUV_{mean} of the whole-body tumor burden by the SUV_{mean} of the parotid glands.⁷ For $qPSG_{mean}$ and $qPSG_{max}$, we observed good reproducibility as well, wCOV was even better than for the uptake values of the parotid gland. Taken together, the high repeatability of uptake in normal organs and for ratios may be relevant for both PSMA-directed imaging and therapy.

Limitations of the study include its low number of patients. Statistical analyses, however, still yielded good stability and correlations in this prospective study. Further, the use of CT-based segmentation for the organs misses a significant number of counts on the PET images that have “bloomed” outside of the CT contours. Relative to PET-based contours, this likely improves repeatability,¹³ although it can be more laborious. In addition, as a possible explanation for the observed differences between both SUV metrics, SUV_{mean} can be impacted by the size of the VOI or the partial volume effect.¹⁴ As such, we also provided information on SUV_{max} , which also provided acceptable repeatability.

Organ	SUV_{max} test	SUV_{max} Retest	r	wCOV	τ
Kidneys ($n = 44$)	55.4 ± 18.8	53.3 ± 18.1	0.83	14.1	0.64
Liver ($n = 22$)	20.4 ± 16.4	18.6 ± 15.2	0.66	47.0	0.55
Spleen ($n = 22$)	15.9 ± 14.3	15.0 ± 15.5	0.81	45.2	0.60
Gll. parotidae ($n = 44$)	18.1 ± 8.3	18.1 ± 6.1	0.83	18.5	0.57
Gll. lacrimales ($n = 42$)*	12.6 ± 5.1	12.9 ± 5.1	0.87	14.4	0.60
Gll. submandibulares ($n = 44$)	19.3 ± 8.0	19.8 ± 8.5	0.98	6.9	0.83

Note: * indicates not assessable in one subject.

TABLE 2 Maximum standardized uptake values (SUV_{max} , given as mean \pm standard deviation) derived from the test and retest scans, correlation coefficients, within-subject coefficient of variation (wCOV, given in %), and Kendall's τ for all normal organs of interest.

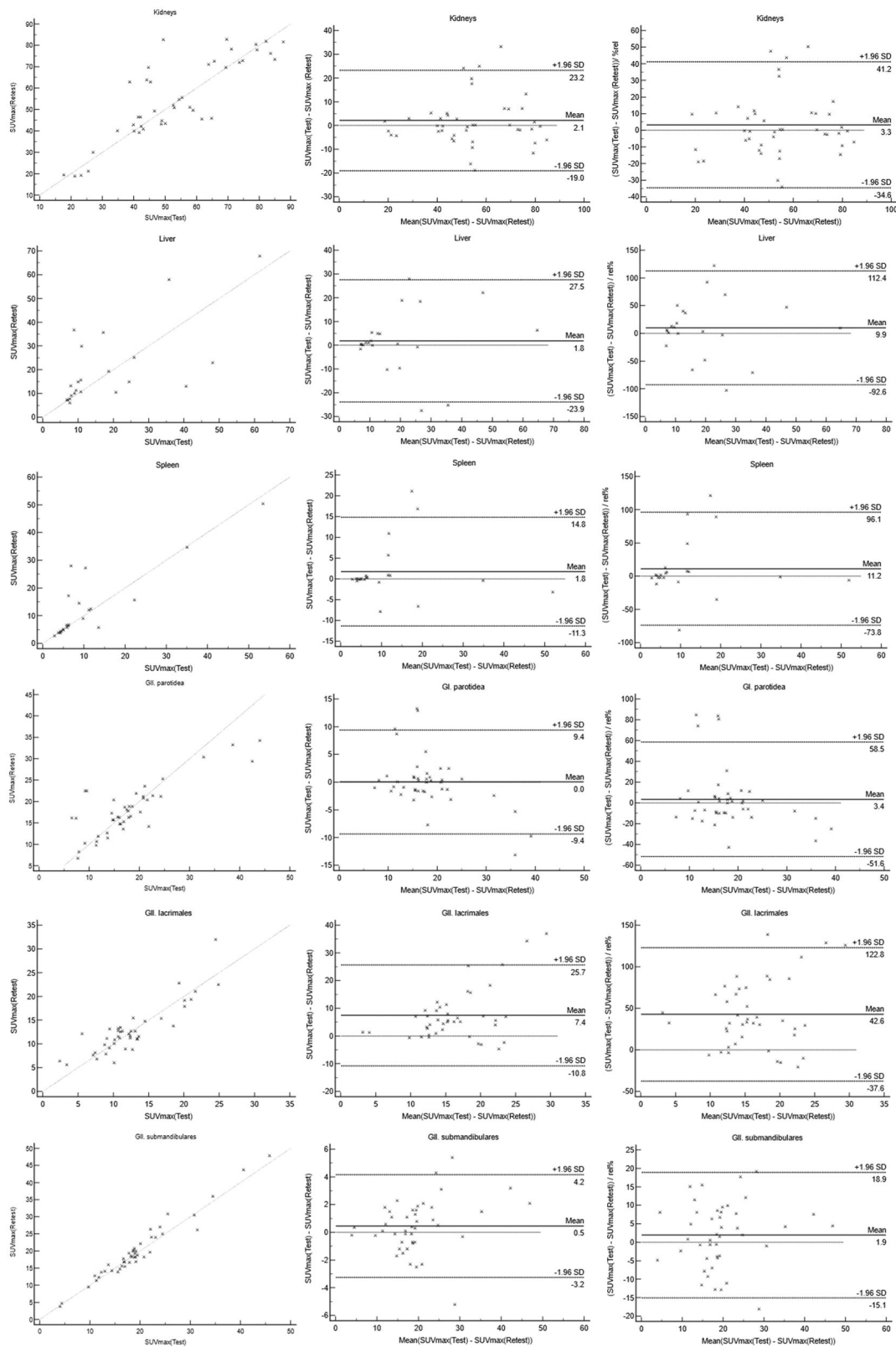


FIGURE 3 Correlations (first column), Bland-Altman plots for absolute (second column) and relative values (third column) of uptake in normal organs for maximum standardized uptake values (SUV_{max}). First row displays the kidneys, second row the liver, third row the spleen, fourth row the lacrimal, fifth row the parotid, and last row the submandibular glands. For smaller organs such as the submandibular glands, absolute and relative values demonstrated lower magnitude of limits, while magnitude of limits were increased for large organs, in particular for the liver.

5 | CONCLUSIONS

We found that ^{18}F -DCFPyL uptake in normal organs is repeatable. As such, the interpreting nuclear medicine specialist can safely rely on proposed reference organs in standardized reporting systems such as PROMISE or E-PSMA. In this regard, SUV_{mean} may be more suitable for larger organs, for example, the liver, which is relevant for standardized PSMA-PET reporting. Beyond scan interpretation, the herein observed repeatability may also have implications for patient selection for PSMA-targeted RLT, as eligible candidates can be identified based on baseline uptake derived from parotid glands (qPSG). The herein observed repeatability for PSG may also lay the groundwork for a more widespread adoption of this ratio in other prospective clinical trials, for example, for evaluation of outcome predictors in patients scheduled for PSMA RLT.

ACKNOWLEDGMENTS

Funding for this study was received from the Movember Foundation, the Prostate Cancer Foundation Young Investigator Award and National Institutes of Health grants CA134675, CA184228, EB024495, and CA183031. This work has been supported by the German Research Foundation (453989101, Takahiro Higuchi, Rudolf A. Werner; 507803309, Rudolf A. Werner), the Okayama University (RECTOR Program, Takahiro Higuchi), and the Japan Society for the Promotion of Science (22H03027, Takahiro Higuchi). Open Access funding enabled and organized by Projekt DEAL.

CONFLICTS OF INTEREST STATEMENT

Martin G. Pomper is a coinventor on a US patent covering ^{18}F -DCFPyL and as such is entitled to a portion of any licensing fees and royalties generated by this technology. This arrangement has been reviewed and approved by the Johns Hopkins University in accordance with its conflict of interest policies. Steven P. Rowe is a consultant for Progenics Pharmaceuticals Inc., the licensee of ^{18}F -DCFPyL. RAB is Consultant for Bayer Healthcare and Eisai GmbH. Ralph A. Bundschuh has a noncommercial research agreement and is on the speakers list with Mediso Medical Imaging (Budapest, Hungary). Rudolf A. Werner received speaker honoraria from Novartis. Markus Essler is Consultant for Bayer Healthcare and Eisai GmbH, IPSEN, and Novartis. The result of this work is part of the doctoral thesis of BH, planned to be submitted at the Medical Faculty of the University of Bonn. The remaining authors declare that there is no conflict of interest as well as consent for scientific analysis and publication.

DATA AVAILABILITY STATEMENT

The data that support the findings of this study are available on request from the corresponding author. The data are not publicly available due to privacy or ethical restrictions.

ORCID

Rudolf A. Werner  <https://orcid.org/0000-0003-3372-6046>

Mark C. Markowski  <http://orcid.org/0000-0003-2780-5100>

Steven P. Rowe  <http://orcid.org/0000-0003-2897-4694>

REFERENCES

- Choyke PL, Bouchelouche K. Prostate specific membrane antigen (PSMA) imaging: the past is prologue. *Transl Androl Urol*. 2019;8:283-285.
- Rowe SP, Buck A, Bundschuh RA, et al. [18F]DCFPyL PET/CT for imaging of prostate cancer. *Nuklearmedizin*. 2022;61:240-246. <https://www.thieme-connect.com/products/ejournals/abstract/10.1055/a-1659-0010>
- Werner RA, Solnes LB, Javadi MS, et al. SSTR-RADS version 1.0 as a reporting system for SSTR PET imaging and selection of potential PRRT candidates: a proposed standardization framework. *J Nucl Med*. 2018;59:1085-1091.
- Ceci F, Oprea-Lager DE, Emmett L, et al. E-PSMA: the EANM standardized reporting guidelines v1.0 for PSMA-PET. *Eur J Nucl Med Mol Imaging*. 2021;48:1626-1638.
- Eiber M, Herrmann K, Calais J, et al. Prostate cancer molecular imaging standardized evaluation (PROMISE): proposed miTNM classification for the interpretation of PSMA-ligand PET/CT. *J Nucl Med*. 2018;59:469-478.
- Werner RA, Bundschuh RA, Bundschuh L, et al. Interobserver agreement for the standardized reporting system PSMA-RADS 1.0 on (18)F-DCFPyL PET/CT imaging. *J Nucl Med*. 2018;59:1857-1864.
- Hotta M, Gafita A, Murthy V, et al. PSMA PET tumor-to-salivary glands ratio (PSG score) to predict response to Lu-177 PSMA radioligand therapy: an international multicenter retrospective study. *J Clin Oncol*. 2022;40:5043.
- Pollard JH, Raman C, Zakharia Y, et al. Quantitative test-retest measurement of (68)Ga-PSMA-HBED-CC in tumor and normal tissue. *J Nucl Med*. 2020;61:1145-1152.
- Jansen BHE, Cysouw MCF, Vis AN, et al. Repeatability of quantitative (18)F-DCFPyL PET/CT measurements in metastatic prostate cancer. *J Nucl Med*. 2020;61:1320-1325.
- Werner RA, Habacha B, Lütje S, et al. High SUVs have more robust repeatability in patients with metastatic prostate cancer: results from a prospective test-retest cohort imaged with (18)F-DCFPyL. *Mol Imaging*. 2022;2022:1-10. <https://clinicaltrials.gov/ct2/show/NCT03793543>. Assessed February 27, 2021.
- Szabo Z, Mena E, Rowe SP, et al. Initial evaluation of [(18)F]DCFPyL for prostate-specific membrane antigen (PSMA)-targeted PET imaging of prostate cancer. *Mol Imaging Biol*. 2015;17:565-574.
- Vicente EM, Lodge MA, Rowe SP, Wahl RL, Frey EC. Simplifying volumes-of-interest (VOIs) definition in quantitative SPECT: beyond manual definition of 3D whole-organ VOIs. *Med Phys*. 2017;44:1707-1717.
- Plyku D, Mena E, Rowe SP, et al. Combined model-based and patient-specific dosimetry for (18)F-DCFPyL, a PSMA-targeted PET agent. *Eur J Nucl Med Mol Imaging* 2018;45:989-998.

How to cite this article: Werner RA, Lütje S, Habacha B, et al. Test-retest repeatability of organ uptake on PSMA-targeted ^{18}F -DCFPyL PET/CT in patients with prostate cancer. *The Prostate*. 2023;83:1186-1192. doi:10.1002/pros.24577